Research Article

INTERNATIONAL JOURNAL OF ADVANCED ROBOTIC SYSTEMS

International Journal of Advanced Robotic Systems
September-October 2016: 1–11

DOI: 10.1177/1729881416662771
arx.sagepub.com
SAGE

Exploiting impedance shaping approaches to overcome force overshoots in delicate interaction tasks

Loris Roveda, Nicola Pedrocchi, and Lorenzo Molinari Tosatti

Abstract

The aim of the presented article is to overcome the force overshoot issue in impedance based force tracking applications. Nowadays, light-weight manipulators are involved in high-accurate force control applications (such as polishing tasks), where the force overshoot issue is critical (i.e. damaging the component causing a production waste), exploiting the impedance control. Two main force tracking impedance control approaches are described in literature: (a) set-point deformation and (b) variable stiffness approaches. However, no contributions are directly related to the force overshoot issue. The presented article extends both such methodologies to analytically achieve the force overshoots avoidance in interaction tasks based on the on-line estimation of the interacting environment stiffness (available through an EKF). Both the proposed control algorithms allow to achieve a linear closed-loop dynamics for the coupled robot-environment system. Therefore, control gains can be analytically on-line calculated to achieve an over-damped closed-loop dynamics of the controlled coupled system. Control strategies have been validated in experiments, involving a KUKA LWR 4+. A probing task has been performed, representative of many industrial tasks (e.g. assembly tasks), in which a main force task direction is defined.

Keywords

Force overshoots avoidance, impedance control, set-point deformation, variable stiffness, interaction tasks, unknown environment estimation

Date received: 5 May 2016; accepted: 15 July 2016

Topic: Special Issue - Manipulators and Mobile Robots
Topic Editor: Michal Kelemen

Introduction

Highly accurate force control is strongly required in many robotic applications.[1–6] Force overshoots might compromise the task execution, resulting in task failures and the production of waste.

Due to their limited inertia and (controlled) compliant behaviour, light-weight manipulators[7] are attractive for the execution of such applications.

Compliant joint manipulators have been investigated for human-robot safe interaction.[8] However, it is still difficult to obtain high-perfomance in force tracking applications involving such robots due to the low rate joint stiffness adaptation and due to the difficulties in compensating for the robot dynamics (such as friction, that is a function of the joint properties). High-perfomance in force tracking applications involving a compliant robot behaviour can be easier achieved by the control side.[9] Since the milestones,[10–12] impedance control[13,14] has been particularly effective in order to interact with compliant environments. In fact, with respect to pure force controllers,[15,16] impedance control compounds an easier tunable dynamic balance response for the robot. In addition, particular design of impedance controllers,[17] grants a wide control bandwidth, thanks to a continuous adaptation of the controller.

ITIA-CNR, Italy

Corresponding author:
Loris Roveda, ITIA-CNR, via Corti 21, Milan, 20133, Italy.
Email: loris.roveda@itia.cnr.it

Nevertheless, some force/deformation regulation requirements are introduced in order to improve the robustness and safety of interaction with a dynamic task, especially in the case of a precision-force process.[18] Although impedance methods have proven to be dynamically equivalent to explicit force controllers,[19] a direct tracking of explicit interaction forces is not straightforwardly allowed.

To perform a tracking of a target force based on the impedance control while preserving the properties of the impedance behaviour (e.g. to simultaneously interact with a human operator), many works have been presented. While some methods are based on the energy tank theory to preserve the passivity of the controlled system,[20,21] and other methods are based on voltage control strategy and can be applied to electrically driven robots[?] (even if no experimental results are shown),[22] many works are directly adapting the impedance control parameters based on the interaction force and can be divided in two main families: class (a) set-point deformation impedance controllers and class (b) variable stiffness controllers. Common solutions of class (a) methods are suggested in the literature[23], where the controlled force is derived from a position control law, scaling the trajectory as a function of the estimated environment stiffness, calculating the time-varying PID gains. Another important approach[24–26] involves the generation of a reference motion as a function of the force-tracking error, under the condition that the environment stiffness is variously unknown, it is estimated as a function of the measured force. Common solutions of class (b) methods consist of gain-scheduling strategies that select the stiffness and damping parameters from a predefined set (off-line calculated) on the basis of the current target state.[27] Lee et al.[28] vary the controlled robot stiffness on-line to regulate the desired contact force based on the previous force tracking error, without any knowledge of the environment. Yang et al.[29] present a human-like learning controller to interact with unknown environments that feed-forward adapts force and impedance. Oh et al.[30,31] describe a frequency-shaped impedance control method which shapes a disturbance observer in the frequency domain so that the impedance is manipulated to achieve both the compliant interaction and reference tracking.

Commonly in class (a) methods, all approaches maintain a constant dynamic behaviour of the controlled robot, so that when the environment stiffness quickly and significantly changes, the bandwidth of the controllers has to be limited to avoid instability, while in class (b) methods, stationary, known and structured environments are considered.

Despite the force overshoots, control is of primary importance in many industrial tasks (e.g. fragile components assembly and polishing), and to the best of the authors' knowledge, few works deal with this issue. In the literature,[32] the authors investigated the possibility of adopting a class (a) controller, while in another case,[33] the authors investigated the possibility of adopting a class (b) controller to guarantee the force overshoots avoidance. Although the experimental validation shows the capabilities of the defined controllers to avoid force overshoots, the authors were not able to analytically calculate the control gains. In Roveda et al.,[34] the authors propose a class (a) optimal controller. However, such control schema relies on the experimental setting of the optimal control gain and of the target force filtering parameters.

The presented article aims to propose and deeply discuss two methodologies, a class (a) control law and a class (b) control law, to analytically overcome the force overshoot issue while tracking a target force, completing the impedance control based state-of-the-art methods. While the class (a) algorithm set-point variation control law has been already described in the literature,[35] the class (b) algorithm proposes a new stiffness adaptation control law to regulate and control the interaction force. The proposed methodologies rely on a common control approach that allows us to shape the equivalent impedance of the coupled *controlled robot–interacting environment* system. Moreover, both of the approaches rely on the estimation of the interacting environment stiffness performed by an extended Kalman filter (EKF). The interaction force measurements are used to track the target force adapting the impedance control parameters. Both the proposed control algorithms allow us to obtain a linear closed-loop coupled robot–environment system. Therefore, control gains can be analytically on-line calculated to achieve an over-damped closed-loop dynamics of the controlled coupled system. Control strategies have been validated in experiments, involving a KUKA LWR 4+ (Figure 1). A probing task has been performed, representative of many industrial tasks (e.g. assembly tasks), in which a main force task direction is defined.

Interacting environment modeling and estimation

Compliant environment dynamics

Denoting $\mathbf{D}_e$ and $\mathbf{K}_e$ as the environment damping and stiffness respectively, a simplified environment dynamics can be modelled[36]

$$\mathbf{f} = -(\mathbf{D}_e\dot{\mathbf{x}}_e + \mathbf{K}_e\,\Delta\mathbf{x}_e) \tag{1}$$

where $\Delta\mathbf{x}_e = \mathbf{x}_e - \mathbf{x}_e^0$, and $\mathbf{x}_e^0$ is the equilibrium position for the environment. In particular, considering a stable contact point with $\mathbf{x}_e^0 = 0$, the environment position is equal to the robot position (i.e. $\mathbf{x}_e = \mathbf{x}_r$), as in Figure 2.

Environment observer design

The environment model in equation (1) is used to implement an EKF for the environment stiffness estimation. Under the mild hypothesis that the contact is preserved once established and simplification hypothesis that the contact(s) are elastic, the robot-environment interaction

is defined by the filter state, augmented with the environment properties

$$\xi_e = [\Delta \mathbf{x}_e, \mathbf{K}_e, \mathbf{D}_e, \mathbf{f}_e]^{\mathrm{T}}. \tag{2}$$

Substituting the augmented state (equation (2)) into the model equation (1), the filter dynamics result in

$$\boldsymbol{f}(\xi_e, \boldsymbol{\nu}_e) = \begin{bmatrix} \mathbf{D}_e^{-1}(-\mathbf{K}_e \Delta \mathbf{x}_e + \mathbf{f}_e + \boldsymbol{\nu}_{\mathbf{x}_e}) \\ \boldsymbol{\nu}_{\mathbf{K}_e} \\ \boldsymbol{\nu}_{\mathbf{D}_e} \\ \boldsymbol{\nu}_{\mathbf{f}_e} \end{bmatrix} \tag{3}$$

where the vector $\boldsymbol{\nu}_e = [\boldsymbol{\nu}_{\mathbf{x}_e}, \boldsymbol{\nu}_{\mathbf{K}_e}, \boldsymbol{\nu}_{\mathbf{D}_e}, \boldsymbol{\nu}_{\mathbf{f}_e}]^{\mathrm{T}}$ accounts for uncertainties in models parameters/estimates.

The observer of the augmented state is therefore defined as

$$\begin{cases} \dot{\hat{\xi}}_e = \boldsymbol{f}(\xi_e, \nu_e) + \mathbf{K}_{EKF}(\mathbf{y} - \mathbf{C}_a \hat{\xi}_e) \\ \hat{\mathbf{y}} = \boldsymbol{H}(\xi_e, w) \end{cases} \tag{4}$$

where $\hat{\xi}$ are estimates, $\mathbf{K}_{EKF}$ is the gain matrix, $\mathbf{C}_a$ is the observation matrix, $\hat{\mathbf{y}}$ is the measurements vector and $H(\xi_e, w)$ is the observation function.

The state $\hat{\xi}$ is updated by measurements of $\mathbf{x}_e$ and $\mathbf{f}_e = \mathbf{f}$,[37] providing the environment stiffness $\hat{\mathbf{K}}_e$ (more details and simulation/experimental validation are shown in the literature.[18])

Impedance control loop

The impedance control loop design has to guarantee a pure decoupled second-order impedance behaviour is achieved for the controlled robot up to a reasonable frequency of around 5 Hz. Such behaviour can be obtained by properly designing a control loop around the standard position controller for many lightweight industrial robots.[38] Therefore, the target dynamics for the controlled robot should result in

$$\mathbf{M}_r \ddot{\mathbf{x}}_r + \mathbf{D}_r \dot{\mathbf{x}}_r + \mathbf{K}_r \Delta \mathbf{x}_r = \mathbf{f}_r, \quad \textit{with} \quad \Delta \mathbf{x}_r := \mathbf{x}_r - \mathbf{x}_r^0 \tag{5}$$

where $\mathbf{x}_r^0$ and $\mathbf{x}_r$ are the desired and actual robot positions respectively, and $\mathbf{f}_r$ is the external interacting force/torque (Figure 2). In addition, the Cartesian stiffness $\mathbf{K}_r$, damping $\mathbf{D}_r$ and mass $\mathbf{M}_r$ have to present negligible extra-diagonal coupling terms with a good approximation up to few Hz. In particular, $\mathbf{D}_r = 2\,\mathbf{h}\,\mathbf{M}_r\,\boldsymbol{\omega}_0$, where $\mathbf{h}$ is diagonal matrix of the imposed damping ratio and $\boldsymbol{\omega}_0 = \sqrt{\mathbf{M}_r^{-1}\mathbf{K}_r}$ is the system pulsation.

Finally, considering a stable contact point with $\mathbf{x}_e^0 = 0$, the environment position is equal to the robot position (i.e. $\mathbf{x}_e = \mathbf{x}_r$) and the force acting on the environment is equal to the force acting on the robot (i.e. $\mathbf{f}_e = \mathbf{f}_r = \mathbf{f}$), as in Figure 2.

Remarkably, the KUKA LWR4+, that is the robot used for the experimental tests, already displays such behaviour as seen in the literature.[9] In fact, experiments show that also $\mathbf{M}_r$ presents negligible extra-diagonal coupling terms with a good approximation up to 5 Hz. Such experimental validation is described by Roveda.[39] In particular, a force input at the robot end-effector has been imposed to the Cartesian impedance controlled KUKA LWR 4+. The applied external force and the Cartesian deformations at the robot end-effector have been measured. The frequency response functions (FRFs) between the external force and the Cartesian positions at the robot end-effector have been therefore estimated, highlighting a decoupled second-order dynamic behaviour for the controlled robot.

Force tracking control algorithms with overshoots avoidance

General notation

$\mathbf{f}$: vector of measured robot forces over the time, considering a stable contact point in which $\mathbf{f} = \mathbf{f}_r = \mathbf{f}_e$

$\mathbf{f}^d$**:** vector of desired robot forces over the time

$\Delta \mathbf{x}_e^d$**:** estimated interacting environment deformation when $\mathbf{f}^d$ is applied, $\Delta \mathbf{x}_e^d = \hat{\mathbf{K}}_e^{-1} \mathbf{f}^d$

$\mathbf{e}_f$**:** tracking force error on-line measured, $\mathbf{e}_f = \mathbf{f}^d - \mathbf{f}$

$\mathbf{K}_{\mathrm{trg}}$**:** target stiffness vector

$\mathbf{K}_0$**:** target stiffness vector at zero-force error

$\mathbf{m}_k$**:** vectors of coefficients corresponding to the slope of the linear map from $\mathbf{e}_f$ to $\mathbf{K}_{\mathrm{trg}}$

$\mathbf{G}_p$: force tracking proportional gain of the contact force loop

$\mathbf{G}_d$: damping derivative gain related to the robot velocity

The main goal of the stable force tracking control problem is related to limiting/eliminating any force overshoot. The problem is therefore formulated taking into account the coupled dynamics (controlled robot–interacting environment) for the established contact with the environment. The algorithms use the estimate of the interacting environment stiffness in order to on-line (analytically) calculate the control gains to achieve target interaction dynamics.

Both the algorithms define a linear variation of the equivalent closed-loop stiffness with respect to the force tracking error, adopting an equivalent control structure. Thus, let us denote $\mathbf{K}_{\mathrm{trg}}$ as the target stiffness the robot would have to display when an external force is applied. A slight different definition of $\mathbf{K}_{\mathrm{trg}}$ is given for the two controllers based on the shaping coefficient $\mathbf{K}_0$ and $\mathbf{m}_k$, defining the stiffness variation of the closed-loop manipulator. In particular, if $\mathbf{m}_k > 0$ the robot stiffness will decrease with $\mathbf{e}_f \to 0$, vice versa if $\mathbf{m}_k < 0$ the robot stiffness will increase with $\mathbf{e}_f \to 0$. This is true only if the force error $\mathbf{e}_f \to 0^+$.

Sections 'Set-point deformation strategy' and 'Variable stiffness strategy' respectively, describe how the stiffness $\mathbf{K}_{\mathrm{trg}}$ is implemented in the set-point deformation strategy and in the variable stiffness strategy.

Set-point deformation strategy

The control law here presented aims at modifying on-line the equivalent stiffness of the closed loop controlled robot acting on the impedance control set-point, in order to avoid the force overshoot when the robot is in contact with the environment.

A simple and suitable formulation for the on-line tuning of the $\mathbf{K}_{\text{trg}}$ is

$$\mathbf{K}_{\text{trg}} = \mathbf{K}_0 + \text{diag}(\mathbf{m}_k)\mathbf{e}_f$$

Thus, we can define two control signal terms $\mathbf{u}_{\text{trg}}$ and $\mathbf{u}_{\text{damp}}$ respectively, designed for displaying the targeted stiffness behaviour and to guarantee the correct closed-loop system damping

$$\mathbf{u}_{\text{trg}} = \text{diag}(\mathbf{K}_{\text{trg}})\,\mathbf{G}_p\Delta\mathbf{x}_e^d$$
$$\mathbf{u}_{\text{damp}} = \mathbf{D}_{\text{add}} = -\mathbf{G}_d\dot{\mathbf{x}}_r$$

Finally, in order to avoid the dependency of the gains from the actual robot configuration (i.e. the stiffness parameter of the Cartesian impedance control), the position set-point $\mathbf{x}_r^0$ to be sent to the LWR4+ controller is imposed to be

$$\mathbf{x}_r^0 = \mathbf{x}_r + \mathbf{K}_r^{-1}\mathbf{u}_{\text{trg}} + \mathbf{u}_{\text{damp}} \tag{6}$$

The control schema, considering the interacting environment observer, is shown in Figure 3.

Closed-loop dynamics

Considering a single DoF (as the impedance control allows to decouple the Cartesian DoF) and substituting the impedance control set-point x_r^0 as defined by equation (6) and the interacting environment dynamics as defined by equation (1) in equation (5), the closed-loop dynamics results as

$$M_r\ddot{x}_r + (D_r + D_e + K_rG_d)\dot{x}_r + (K_e + G_pm_kf^d)x_r = G_pf^dK_e^{-1}(K_0 + m_kf^d) \tag{7}$$

By imposing the equivalent closed-loop system mass as $M_{\text{eq}} = M_r$, the equivalent closed-loop system damping as $D_{\text{eq}} = D_r + D_e + K_rG_d$, the equivalent closed-loop stiffness as $K_{\text{eq}} = K_e + G_pm_kf^d$ and $f_{\text{eq}} = G_pf^dK_e^{-1}(K_0 + m_kf^d)$, it is possible to analytically calculate the resulting robot base position during the interaction

$$x_r(t) = c_1e^{t\lambda_1} + c_2e^{t\lambda_2} + \frac{f_{\text{eq}}}{K_{\text{eq}}} \tag{8}$$

where

$$\lambda_{1,2} = \frac{-D_{\text{eq}} \pm \sqrt{\Delta_{\text{eq}}^2 - 4_{\text{eq}}K_{\text{eq}}}}{2M_{\text{eq}}} \tag{9}$$

are the eigenvalues of the coupled controlled system (equation (7)) and the constants c_1 and c_2 depends on the initial position $x_{r,0}$ and velocity $\dot{\mathbf{x}}_{r,0}$ conditions, easily calculated by imposing $x_r(0) = x_{r,0}$ and $\dot{\mathbf{x}}_r(0) = \dot{\mathbf{x}}_{r,0}$.

Control parameters calculation

The control parameters G_p and G_d can be calculated analytically in order to guarantee the proper force tracking during the task execution, while avoiding any force overshoot.

G_p gain can be calculated considering the static term of equation (7). In fact, at the steady state, the robot position has to be equal to $x_r = f^d/K_e$ in order to have a zero steady state force error (i.e. the penetration of the robot in the interacting environment $x_e = x_r$ results in the target force f^d). Therefore, the proportional gain G_p results in the following

$$K_{\text{eq}}\frac{f^d}{K_e} = f_{\text{eq}} \rightarrow G_p = \frac{K_e}{K_0} \tag{10}$$

Substituting equation (10) into equation (6) it is possible to calculate the control signal terms u_{trg}, defining the variable stiffness of the controlled robot as

$$u_{\text{trg}} = \text{diag}(K_{\text{trg}})\,K_0^{-1}f^d = \text{diag}(K_0 + \text{diag}(m_k)e_f)\,K_0^{-1}f^d$$

Therefore, the control signal term u_{trg} is not a function of the estimated interacting environment stiffness $\hat{K}_e$. Therefore, the method allows us to obtain zero steady state force error even with errors in the estimation of the interacting environment stiffness.

G_d gain can be calculated considering the eigenvalues in equation (9). In fact, by properly defining such derivative gain it is possible to obtain an over-damped system, allowing us to avoid any force overshoot during the task execution. In particular, to have an over-damped system, the following inequality has to be satisfied

$$D_{\text{eq}}^2 - 4M_{\text{eq}}K_{\text{eq}} > 0 \tag{11}$$

In such a way, the eigenvalues in equation (9) are negative real ($D_{\text{eq}} > \sqrt{4M_{\text{eq}}K_{\text{eq}}}\,\forall$ set of physical parameters). Therefore, considering the worst interaction condition (i.e. interacting environment damping is considered $D_e = 0$), the derivative gain G_d can be calculated as

$$G_d = \frac{\sqrt{4M_{\text{eq}}(G_pm_kf^d + K_e)} - D_r}{K_r} \tag{12}$$

Such definition allows us to obtain an over-damped system and avoid any force overshoot.

The control gain G_d is a function of the impedance parameters M_r, D_r, K_r, of the control parameters G_p, m_k, of the target force f^d, and of the estimated stiffness of the interacting environment K_e. Moreover, even if equation (12) allows us to calculate the derivative control gain G_d considering a zero initial velocity $\dot{\mathbf{x}}_{r,0} = 0$, equation (8) can be used to numerically calculate the derivative gain, taking into account a non-zero initial velocity to avoid any force overshoot in the contact phase.

Based on equation (12), control parameters m_k and K_0 do not affect the force overshoots avoidance, while they affect the closed-loop bandwidth. In fact, their values define the eigenvalues in equation (9).

It has to be highlighted that if the interacting environment mass M_e has to be taken into account, the equivalent mass results in $M_{\text{eq}} = M_r + M_e$. In such a way, the formulation is still valid and the control parameters can be selected to achieve target dynamics of the closed-loop coupled system.

Variable stiffness strategy

The control law here presented aims at modifying on-line the equivalent stiffness of the closed loop controlled robot directly acting on the impedance control stiffness, in order to avoid the force overshoot when the robot is in contact with the environment.

A simple and suitable formulation for the on-line tuning of the $\mathbf{K}_{\text{trg}}$ is

$$\mathbf{K}_{\text{trg}} = \mathbf{K}_0 + \text{diag}(\mathbf{m}_k)\,\text{diag}(\mathbf{f}^d)^{-1}\mathbf{e}_f$$

Thus, we can directly define the impedance control stiffness as

$$\begin{aligned}\mathbf{K}_r &= \text{diag}(\mathbf{K}_{\text{trg}}) - \text{diag}(\mathbf{D}_{\text{add}}) \\ &= \text{diag}(\mathbf{K}_{\text{trg}}) - \text{diag}(\mathbf{G}_p^{-1}\,\mathbf{G}_d\,\text{diag}(\Delta\mathbf{x}_e^d)^{-1}\,\dot{\mathbf{x}}_r)\end{aligned} \tag{13}$$

The $\mathbf{D}_{\text{add}}$ term is used to increase the damping of the closed-loop system. The position set-point $\mathbf{x}_r^0$ to be sent to the LWR4+ controller is imposed to be

$$\mathbf{x}_r^0 = \mathbf{x}_r + \mathbf{G}_p\Delta\mathbf{x}_e^d \tag{14}$$

The control schema, considering the interacting environment observer, is shown in Figure 4.

Closed-loop dynamics

Considering a single DoF (as the impedance control allows to decouple the Cartesian DoF) and substituting the impedance control set-point x_r^0 as defined by equation (14), the impedance control stiffness as defined by equation (13) and the interacting environment dynamics as defined by equation (1) in equation (5), the closed-loop dynamics results as

$$\begin{aligned}&M_r\,\ddot{x}_r + (D_r + D_e)\dot{x}_r \\ &\quad + (K_e + K_{\text{trg}} - D_{\text{add}})(x_r - x_r - G_p\Delta x_e^d) = 0\end{aligned}$$

By elaborating such expression we obtain

$$\begin{aligned}&M_r\,\ddot{x}_r + (D_r + D_e + G_d)\dot{x}_r + (K_e + G_p m_k)x_r \\ &\quad = G_p f^d K_e^{-1}(K_0 + m_k)\end{aligned} \tag{15}$$

By imposing the equivalent closed-loop system mass as $M_{\text{eq}} = M_r$, the equivalent closed-loop system damping as $D_{\text{eq}} = D_r + D_e + G_d$, the equivalent closed-loop stiffness as $K_{\text{eq}} = K_e + G_p m_k$ and $f_{\text{eq}} = G_p f^d K_e^{-1}(K_0 + m_k)$, it is possible to analytically calculate the resulting robot base position during the interaction as described in Section 'Set-point deformation strategy: Closed-loop dynamics' by equation (8).

Control parameters calculation

The control parameters G_p and G_d can be calculated analytically in order to guarantee the proper force tracking during the task execution, while avoiding any force overshoot.

As described in Section 'Set-point deformation strategy: Control parameters calculation', G_p gain can be calculated considering the static term of equation (15). Therefore, the proportional gain G_p results in the following

$$K_{\text{eq}}\frac{f^d}{K_e} = f_{\text{eq}} \rightarrow G_p = \frac{K_e}{K_0} \tag{16}$$

Substituting equation (16) into equation (14) it is possible to highlight that the impedance control set-point is not a function of the environment stiffness estimation ($x_r^0 = x_r + G_p f^{d^{-1}}$).

G_d gain can be calculated considering the eigenvalues in equation (9) as in Section 'Set-point deformation strategy: Control parameters calculation' to obtain an over-damped closed-loop system

$$G_d = \sqrt{4M_{\text{eq}}(G_p m_k + K_e)} - D_r \tag{17}$$

Such definition allows us to obtain an over-damped system and avoid any force overshoot.

The control gain G_d is a function of the impedance parameters M_r, D_r, K_r, of the control parameters G_p, m_k, of the target force f^d, and of the estimated stiffness of the interacting environment K_e. Moreover, even if equation (17) allows us to calculate the derivative control gain G_d considering a zero initial velocity $\dot{\mathbf{x}}_{r,0} = 0$, equation (8) can be used to numerically calculate the derivative gain taking into account a non-zero initial velocity to avoid any force overshoot in the contact phase.

Based on equation (17), control parameters m_k and K_0 do not affect the force overshoots avoidance, while they affect the closed-loop bandwidth. In fact, their values define the eigenvalues in equation (9).

It has to be highlighted that if the interacting environment mass M_e has to be taken into account, the equivalent mass results in $M_{\text{eq}} = M_r + M_e$. In such a way, the formulation is still valid and the control parameters can be selected to achieve target dynamics of the closed-loop coupled system.

Free-motion approach velocity controller

As described in 'Set-point deformation strategy: Control parameters calculation' and in 'Variable stiffness strategy:

Control parameters calculation', the derivative gain G_d can be calculated to take into account non-zero approach velocities for both the proposed control strategies. Thus, it is possible to avoid any force overshoot even if the robot has to perform multiple non-contact to contact phases. In more detail, for the free-space motion it is possible to define a velocity control loop to approach the target environment with a target velocity as follows (considering 1 DoF)

$$x_r^0 = x_r + G_v\,(\dot{x}_r^d - \dot{x}_r) \tag{18}$$

where G_v is the velocity control gain and $\dot{x}_r^d$ is the target approach velocity. Based on the target approach velocity $\dot{\mathbf{x}}_r^d$, it is then possible to calculate the control gain G_d to avoid any force overshoot in the following contact phase.

Therefore, considering the free-space motion, control gains are imposed $G_p = 0$, $G_d = 0$, while considering the contact phase $G_v = 0$. During the impact collision, the target approach velocity is set $\dot{\mathbf{x}}_r^d = 0$ and a logistic function can be used in order to adapt the control gains values G_v, G_p, G_d. Such continuous and differentiable function guarantees, indeed, a smooth control action during the control gains switching. Therefore, the generic control gain G_{ith} during the impact collision results in

$$G_{\text{ith}}^{\text{impact}}(t) = \frac{G_{\text{ith}}^{\text{contact}} - G_{\text{ith}}^{\text{free-space}}}{1 + \exp^{-(t-\bar{t})/\tau_{\text{ith}}}} + G_{\text{ith}}^{\text{free-space}} \tag{19}$$

where τ_{ith} is the time constant of the control gain adaptation. The dynamics of the logistic functions is faster than the dynamics of the observer and of the control loop (at least 1 decade). Therefore, the analytical control gains adaptation defined in Section 'Set-point deformation strategy' and in Section 'Variable stiffness strategy' will not be affected by the logistic function dynamics.

Experimental results

All of the quantities are referred to the robot base reference frame. The impedance loop rate is 200 Hz, synchronously with the environment estimation. In fact, the KUKA LWR 4+ allows us to tune such control loop rate.[9] Signals are updated to the main LWR 4+ control loop, together with the sampling of force (used in the control loop and by the EKF) and the kinematics state. The remote controller is a real-time Linux Xenomai PC with RTNet.

The coupled environment is implemented using a second KUKA LWR 4+ (see Figure 1), setting $K_{e,z} = K_{r,z}^{\text{robot2}} = 20000N/m$, obviously *without* injecting known parameters K_e into the controller instead of observations. Such equivalent stiffness has been obtained with the position control loop of the KUKA LWR 4+. In fact, assuming small Cartesian deformations, it is possible to consider the position controlled KUKA LWR 4+ equivalent to a second order system with the above equivalent stiffness.[39]

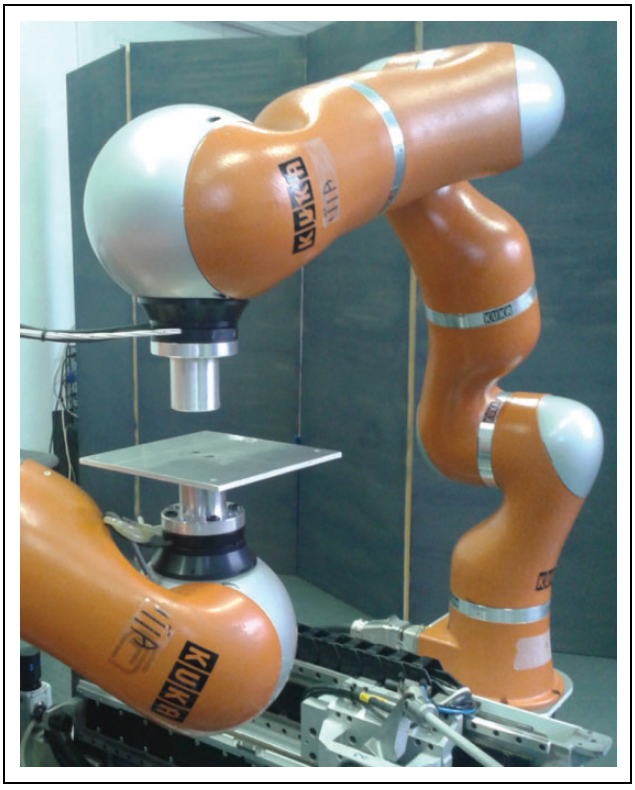

Figure 1. Experimental set-up. One KUKA LWR4+ is used as a variable stiffness environment. The second KUKA LWR4+ implements the optimal impedance force-tracking controller described in the article.

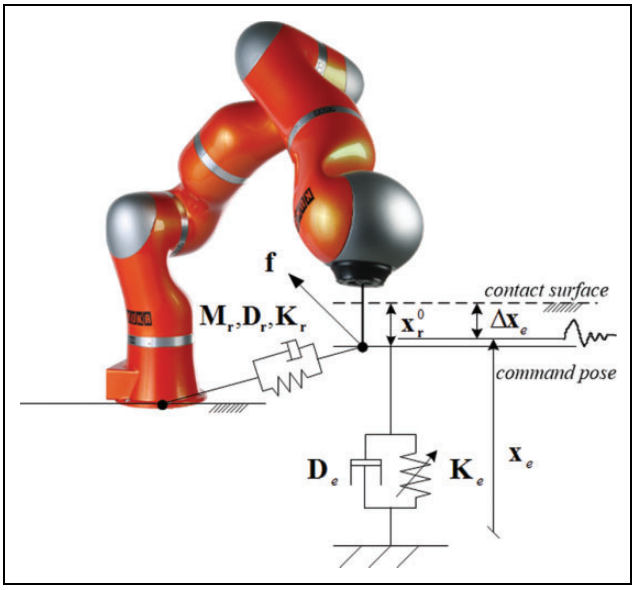

Figure 2. KUKA LWR 4 + interaction model.

Set-point deformation strategy

Control gains has been imposed as follows: $K_{0,z} = 5000$ N/m, $m_{k,z} = 500$ 1/m, while the impedance stiffness $K_{r,z} = 2500$ N/m and the impedance damping ratio $h_z = 0.5$.

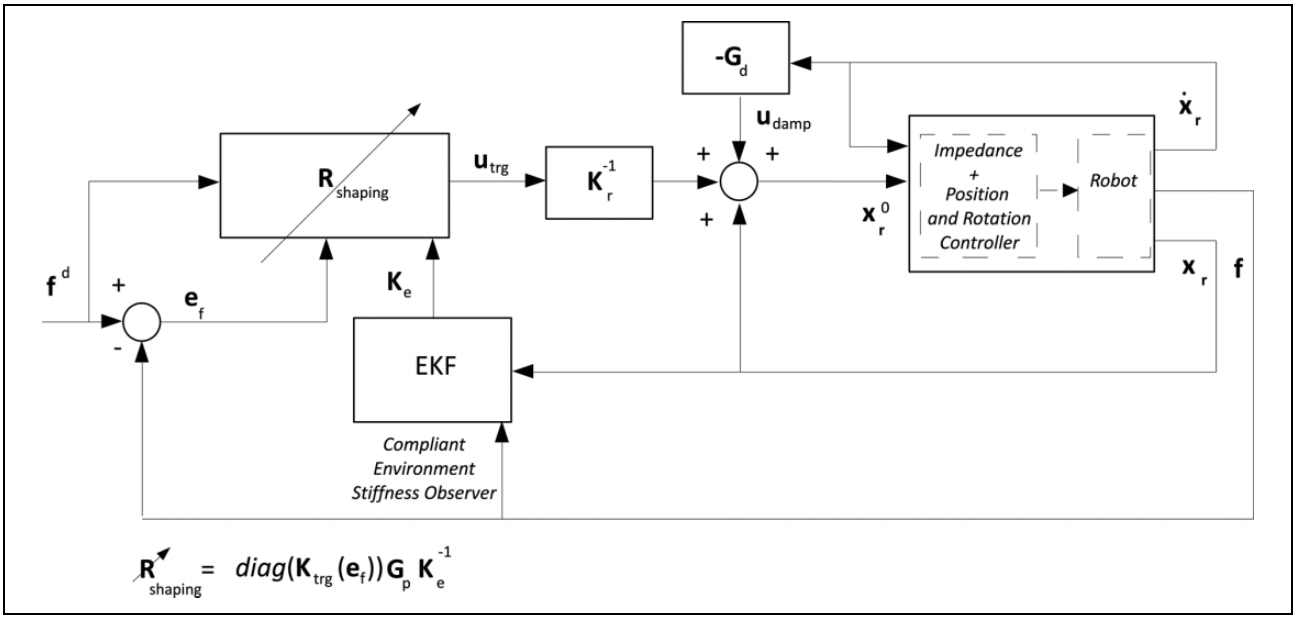

Figure 3. Set-point deformation control schema, including the interacting environment observer (EKF).

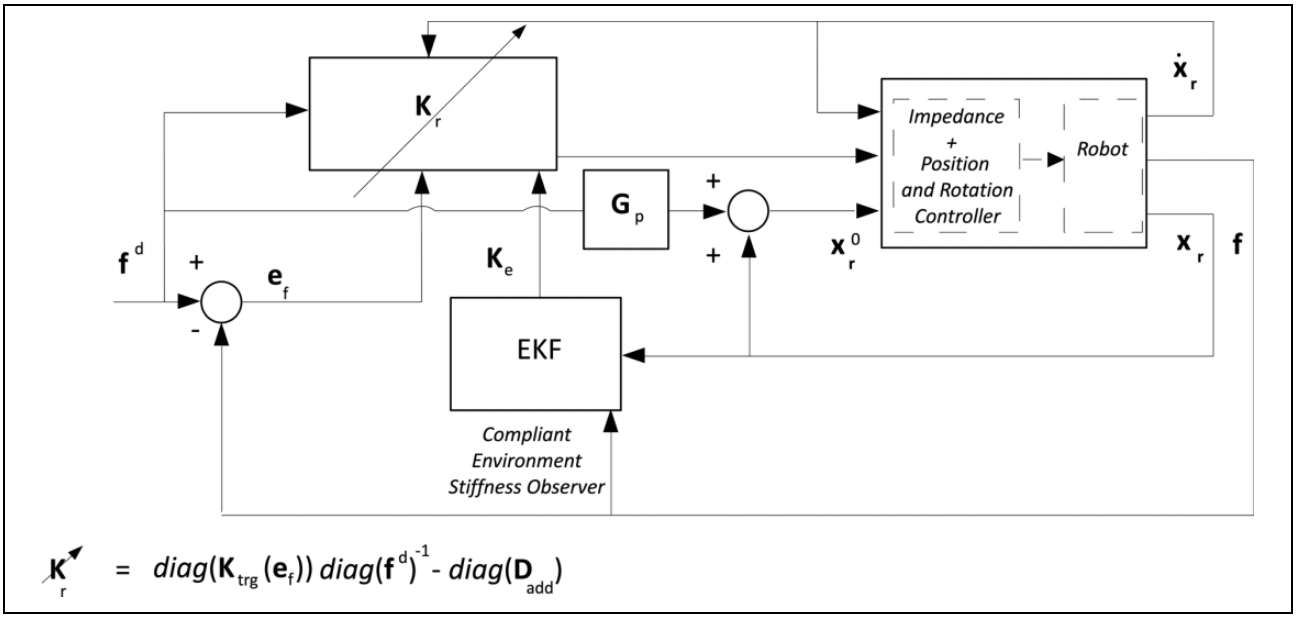

Figure 4. Variable stiffness control schema, including the interacting environment observer (EKF).

Figure 5(a) shows the measured force during the interaction task execution using the set-point deformation control algorithm. Force overshoots are avoided and the proper force tracking is achieved. In fact, the force error is less than 1 % (i.e. negligible force error), attributable to non-compensated dynamic, as static friction. Figure 5(b) shows the estimated environment stiffness during the task execution. Figure 5(c) shows the measured $x_{r,z}$ and commanded $x^0_{r,z}$ robot positions.

Variable stiffness strategy

Control gains has been imposed as follows: $K_{0,z} = 2000$ [N/m], $m_{k,z} = 2000$ [N/m], while the impedance damping ratio $h_z = 0.5$. Figure 6(a) shows the measured force during the interaction task execution using the variable stiffness control algorithm. Force overshoots are avoided and the proper force tracking is achieved. In fact, the force error is less than 1 % (i.e. negligible force error), attributable to non-compensated dynamic, as static friction. Figure 6(b) shows the estimated environment stiffness during the task

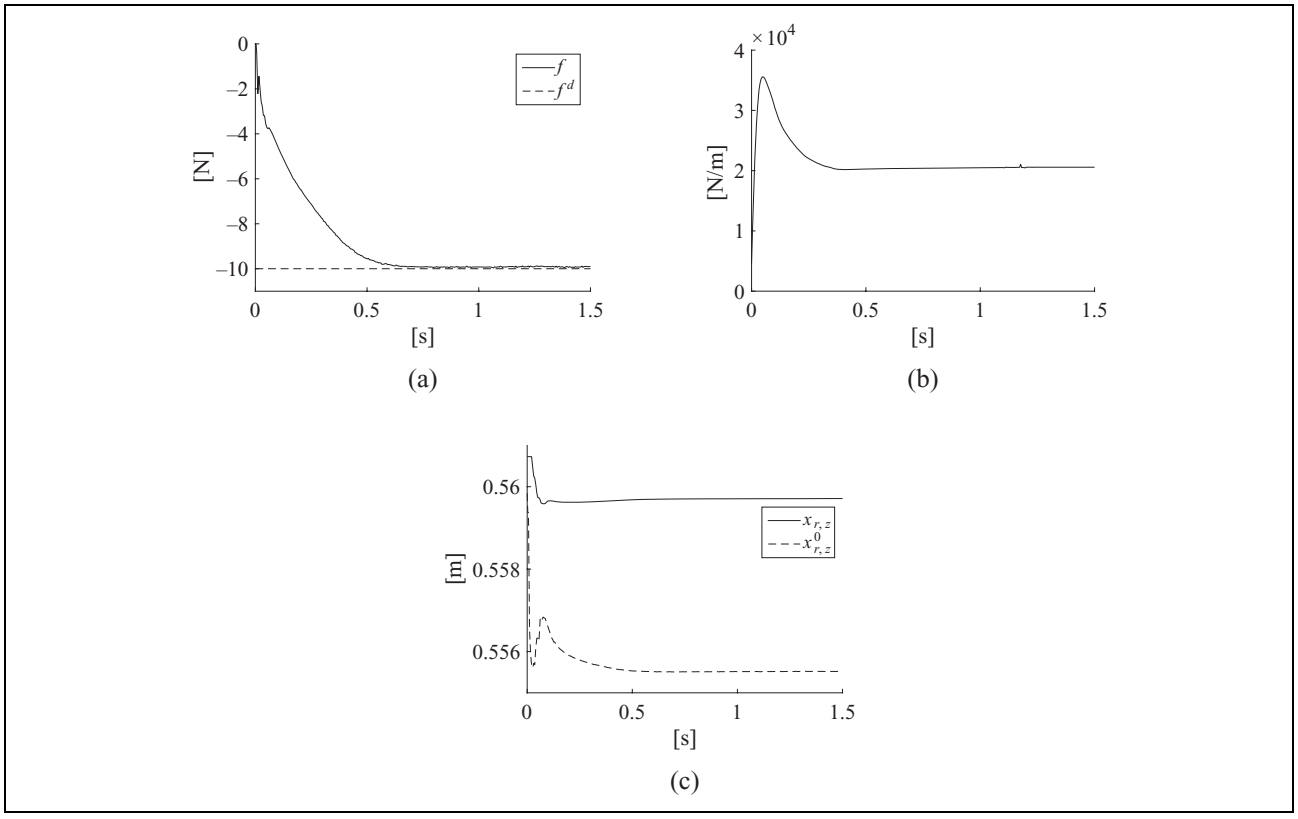

Figure 5. Set-point deformation approach. (a) Interaction target and measured forces are shown. (b) Estimated environment stiffness is shown. (c) Robot measured $x_{r,z}$ and commanded $x^0_{r,z}$ position.

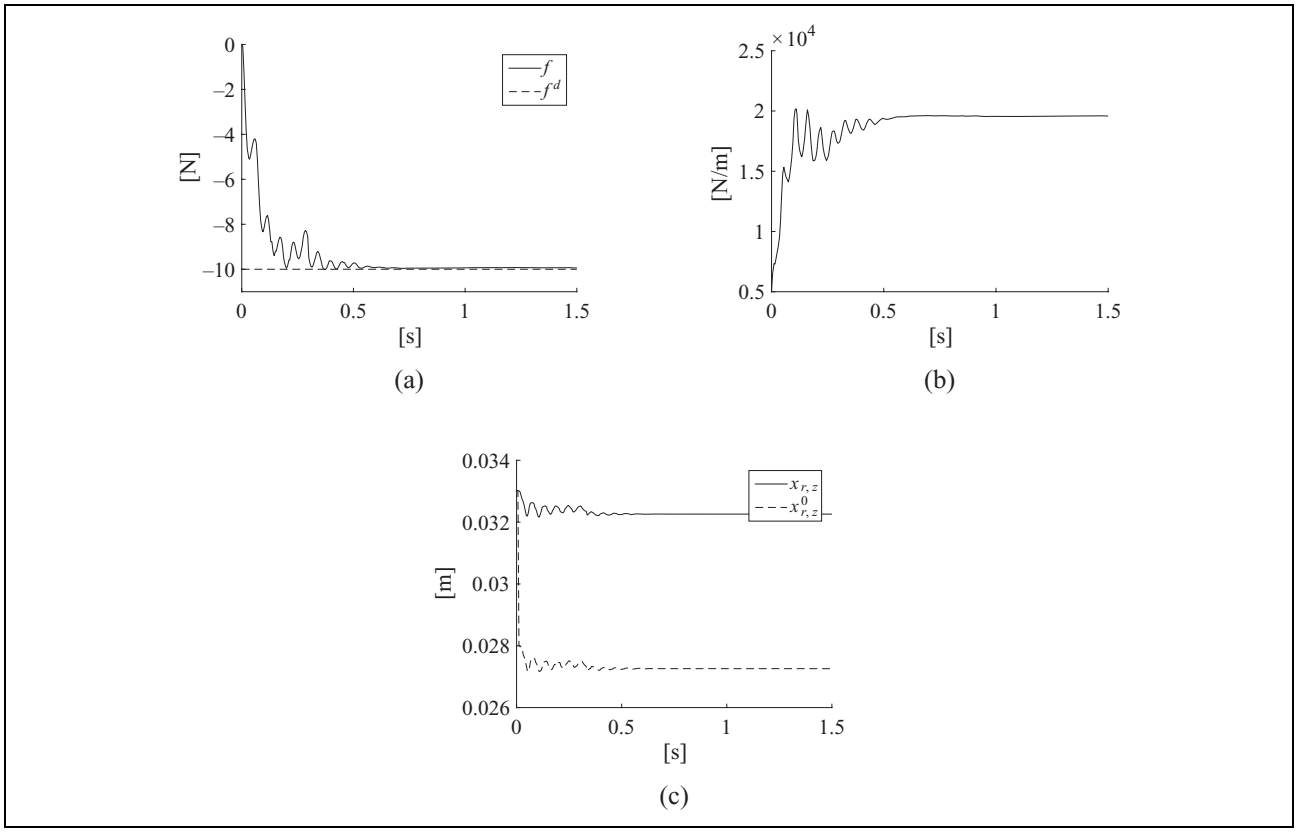

Figure 6. Variable stiffness approach. (a) Interaction target and measured forces are shown. (b) Estimated environment stiffness is shown. (c) Robot measured $x_{r,z}$ and commanded $x^0_{r,z}$ position.

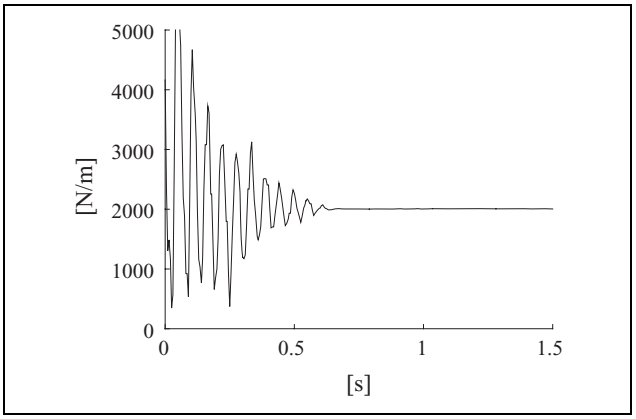

Figure 7. Variable stiffness approach. Impedance control stiffness $K_{r,z}$ during the task execution.

execution. Figure 6(c) shows the measured $x_{r,z}$ and commanded $x^0_{r,z}$ robot positions.

Figure 7 shows the impedance control stiffness $K_{r,z}$ calculated and commanded during the task execution. Since KUKA LWR 4+ impedance control allows us to impose a stiffness in the range [0, 5000] N/m,[9] the maximum stiffness is saturated at 5000 N/m. Only one oscillation is saturated. To avoid such behaviour control parameters can be tuned to reduce the control bandwidth.

Methods comparison

Since a common structure has been adopted for both the control strategies (i.e. both of the control strategies (a) and (b) rely on the definition of an equivalent stiffness $\mathbf{K}_{\text{trg}}$ – as a function of the force error $\mathbf{e}_f$ – and of an equivalent damping $\mathbf{D}_{\text{add}}$ – as a function of the robot velocity $\dot{\mathbf{x}}_r$), the same performance can be achieved by the two controllers by properly imposing the control gains. The main limitations of the class (a) control strategy are related to the maximum admissible $\Delta\mathbf{x}_r^{\max}$ (considering the KUKA LWR 4+ $\Delta\mathbf{x}_r^{\max} = 0.2$ m[9]), while the main limitations of the class (b) control strategy are related to the admissible range of the impedance control stiffness (considering the KUKA LWR 4+ the stiffness can be imposed in the range [0, 5000] N/m[9]) and to the admissible loop rate for the impedance control stiffness adaptation. The developed class (a) method therefore, is more feasible for high-accurate interaction with stiff and delicate components (such as polishing) having a higher range of achievable dynamics, while the developed class (b) method is more feasible for interaction with compliant components (such as assembly of plastic components), since the impedance control behaviour can be tune at low stiffness values to reject disturbances, imposing a limited bandwidth to the controlled robot.

Both of the approaches allow us to obtain the tracking of the target force with a zero-steady-state force error as shown in 'Set-point deformation strategy: Control parameters calculation' and in 'Variable stiffness strategy: Control parameters calculation', even if estimation errors are affecting the environment stiffness estimate $\hat{\mathbf{K}}_e$. In fact, in the case of an environment stiffness over-estimate, both the algorithms allow us to obtain an over-damped behaviour on the basis of equation (12) and equation (17), while in the case of an environment stiffness under-estimate, since in the theoretical analysis the environment damping is $\mathbf{D}_e = \mathbf{0}$, small errors resulting from the EKF[18] are not resulting in force overshoots. In order to be more conservative, the impedance control damping can be also considered $\mathbf{D}_r = 0$ in the theoretical analysis to compensate for estimation errors affecting the environment stiffness estimate $\hat{\mathbf{K}}_e$.

Conclusions

The described article proposes two control algorithms (a set-point deformation algorithm and a variable stiffness algorithm) to overcome the force overshoot issue in impedance based force tracking control, completing the state-of-the-art methods. Both of the algorithms rely on a common control law to shape the equivalent impedance of the coupled *controlled robot–interacting environment* system (the interaction force is used to regulate the closed-loop stiffness of the controlled manipulator) and on the estimation of the environment stiffness performed by an EKF. In such a way, control gains can be analytically on-line calculated to achieve an over-damped closed-loop dynamics of the controlled coupled system. Control strategies have been validated in experiments, involving a KUKA LWR 4+. A probing task has been performed, representative of many industrial tasks (e.g. assembly tasks) in which a main force task direction is defined. Future work will investigate the possibility of extending the proposed approach to rotational degrees of freedom and will consider the application of such control algorithms to a direct human-robot cooperation in interaction tasks.

Declaration of conflicting interests

The author(s) declared no potential conflicts of interest with respect to the research, authorship, and/or publication of this article.

Funding

The author(s) disclosed receipt of the following financial support for the research, authorship and/or publication of this article: The work has been developed within the project European Robotic Challenge, funded from European Unions Seventh Framework Programme under grant agreement n. 608849.

References

1. Doggett D. Robotic assembly of truss structures for space systems and future research plans. In: *Aerospace conference proceedings*, Big Sky, Montana, 9–16 March 2002, vol.7, pp.7–3589. IEEE.
2. Márquez JJ, Pérez JM, Rıos J, et al. Process modeling for robotic polishing. *J Mater Process Technol* 2005; 159: 69–82.
3. Rembala R and Ower C. Robotic assembly and maintenance of future space stations based on the iss mission operations experience. *Acta Astron* 2009; 65: 912–920.

4. Tsai MJ, Huang JF and Kao WL. Robotic polishing of precision molds with uniform material removal control. *Int J Mach Tool Manu* 2009; 49: 885–895.
5. Pirrotta S. Preliminary study on a novel coring system for planetary surface sampling: *Proceedings of the 7th international planetary probe workshop*, Barcelona, Spain, 14–18 June 2010, pp.14–18. Paris: European Space Agency.
6. Zhang LJ, Hu RQ, Yi WM, et al. A study of flexible force control method on robotic assembly for spacecraft. In: *Applied mechanics and materials*, Trans Tech Publ: Churerstrasse 20, CH-8808 Pfaffikon, Switzerland, 2014, vol.681, pp.79–85.
7. Stolt A, Linderoth M, Robertsson A, et al. Robotic assembly of emergency stop buttons. In: *Intelligent robots and systems (IROS), 2013 IEEE/RSJ int conf on*, Tokyo, Japan, 03–07 November 2013, pp.2081–2081. IEEE: Tokyo Big Sight.
8. Rethink. Baxter research robot (visited January 2015), June 2012 founded in 2008, Boston, Massachusetts, USA.
9. Albu-Schäffer A, Ott C and Hirzinger G. A unified passivity-based control framework for position, torque and impedance control of flexible joint robots. *Int J Robot Res* 2007; 26: 23–39.
10. Salisbury JK. Active stiffness control of a manipulator in cartesian coordinates. In: *Decision and control including the symposium on adaptive processes, 1980 19th IEEE conference on*, Albuquerque, New Mexico, 10–12 December 1980, vol.19, pp.95–100. Institute of Electrical and Electronics Engineers.
11. Mason MT. Compliance and force control for computer controlled manipulators. *IEEE Transactions on Systems, Man, and Cybernetics* 1981; 11(6): 418–432.
12. Raibert MH and Craig JJ. Hybrid position/force control of manipulators. *Journal of Dynamic Systems, Measurement, and Control* 1981; 103(2): 126–133.
13. Hogan N. Impedance control: An approach to manipulation. In *American Control Conference, 1984*, San Diego, CA, 6–8 June 1984, pp.304–313.
14. Colgate E and Hogan N. An analysis of contact instability in terms of passive physical equivalents. In *Robotics and automation (ICRA), 1989 IEEE int conf on*, Scottsdale, AZ, 14–19 May 1989, pp.404–409. IEEE.
15. Lange F, Jehle C, Suppa M, et al. Revised force control using a compliant sensor with a position controlled robot. In: *Robotics and automation (ICRA), 2012 IEEE int conf on*, Minneapolis, MN, 14–18 May 2012, pp.1532–1537. IEEE.
16. Lange F, Bertleff W and Suppa M. Force and trajectory control of industrial robots in stiff contact. In: *Robotics and automation (ICRA), 2013 IEEE int conf on*, Karlsruhe, Germany, 6–10 May 2013, pp.2927–2934. IEEE.
17. Ott C, Mukherjee R and Nakamura Y. Unified impedance and admittance control. In: *Robotics and automation (ICRA), 2010 IEEE int conf on*, Anchorage, AK, 3–8 May 2010, pp. 554–561. IEEE.
18. Roveda L, Vicentini F and Tosatti LM. Deformation-tracking impedance control in interaction with uncertain environments. In: *Intelligent robots and systems (IROS), 2013 IEEE/RSJ int conf on*, Tokyo, Japan, 3–7 November 2013, pp.1992–1997. IEEE.
19. Volpe R and Khosla P. The equivalence of second-order impedance control and proportional gain explicit force control. *Int J Robot Res* 1995; 14: 574–589.
20. Ferraguti F, Secchi C and Fantuzzi C. A tank-based approach to impedance control with variable stiffness. In: *Proceedings of the 2013 int conf on robotics and automation (ICRA)*, Karlsruhe, Germany, 6–10 May 2013, pp.2927–2934. IEEE.
21. Schindlbeck C and Haddadin S. Unified passivity-based cartesian force/impedance control for rigid and flexible joint robots via task-energy tanks. In: *IEEE International Conference on Robotics and Automation (ICRA)*, Seattle, WA, 26–30 May 2015. IEEE.
22. Mehdi FM and Fateh BR. Impedance control of robots using voltage control strategy. *Nonlinear Dynamics, Springer* 2013; 74(1–2): 277–286.
23. Villani L, Canudas de Wit C and Brogliato B. An exponentially stable adaptive control for force and position tracking of robot manipulators. *IEEE Trans Automat Contr* 1999; 44: 798–802.
24. Seraji H and Colbaugh R. Adaptive force-based impedance control. In: *Intelligent robots and systems' 93, IROS'93. Proceedings of the 1993 IEEE/RSJ int conf on*, Yokohama, Japan, 26–30 July 1993, vol.3, pp.1537–1544. IEEE.
25. Seraji H and Colbaugh R. Force tracking in impedance control. *Int J Robot Res* 1997; 16: 97–117.
26. Jung S, Hsia TC and Bonitz RG. Force tracking impedance control of robot manipulators under unknown environment. *IEEE Trans Contr Syst Technol* 2004; 12: 474–483.
27. Ikeura R and Inooka H. Variable impedance control of a robot for cooperation with a human. In *Robotics and automation (ICRA), 1995 IEEE int conf on*, Nagoya, Japan, 21–27 May 1995, vol.3, pp.3097–3102. IEEE.
28. Lee K and Buss M. Force tracking impedance control with variable target stiffness. *The International Federation of Automatic Control* 2000; 16: 6751–6756. Elsevier.
29. Yang C, Ganesh G, Haddadin S, et al. Human-like adaptation of force and impedance in stable and unstable interactions. *IEEE Trans Robot* 2011, 27: 918–930.
30. OH S, WOO H and Kong K. Frequency-shaped impedance control for safe human -robot interaction in reference tracking application. *IEEE/ASME Transactions on Mechatronics* 2014; 19(6): 1907–1916.
31. Oh S, Woo H and Kong K. Stability and robustness analysis of frequency-shaped impedance control for reference tracking and compliant interaction. In: *World congress*, Cape Town International Convention Centre, 24–29 August 2014, vol.19, pp.3557–3562.
32. Roveda L, Vicentini F, Pedrocchi N, et al. Force-tracking impedance control for manipulators mounted on compliant bases. In: *Robotics and automation (ICRA), 2014 IEEE int conf on*, Hong Kong, China, 31 May–5 June 2014. IEEE.
33. Roveda L, Vicentini F, Pedrocchi N, et al. Impedance shaping controller for robotic applications in interaction with compliant

environments. In: *Informatics in control, automation and robotics, 2014 11th int conf on*, Vienna, Austria, 01–03 September 2014, vol.2, pp.444–450. IEEE.
34. Roveda L, Iannacci N, Vicentini F, et al. Optimal impedance force-tracking control design with impact formulation for interaction tasks. *IEEE Robotics and Automation Letters* 2016, 1: 130–136.
35. Roveda L, Vicentini F, Pedrocchi N, et al. Impedance control based force-tracking algorithm for interaction robotics tasks: an analytically force overshoots-free approach. In: *Informatics in Control, Automation and Robotics*, Colmar, Alsace, France, 21–23 July 2015. IEEE.
36. Flügge W. *Viscoelasticity*. New York: Springer, 1975.
37. Haykin SS, ed. *Kalman filtering and neural networks*. New York: Wiley, 2001.
38. Siciliano B and Villani L. *Robot force control. 1st ed*. Norwell, MA: Kluwer Academic Publishers, 2000.
39. Roveda L. *Model based compliance shaping control of lightweight manipulator in hard-contact industrial applications*. PhD Thesis, Politecnico di Milano, Italy, 2015.